M. Eisencraft, R. Attux and R. Suyama (Eds.)

Chaotic Signals in Digital Communications

Contents

5

Basics of Communications Using Chaos

Géza Kolumbán

Pázmány Péter Catholic University, Budapest, Hungary

Tamás Krébesz

Budapest University of Technology and Economics, Hungary

Chi Kong Tse

The Hong Kong Polytechnic University, Hong Kong SAR, China

Francis C. M. Lau

The Hong Kong Polytechnic University, Hong Kong SAR, China

CONTENTS

In digital communications, either fixed, chaotic or random, analog waveforms of finite duration are used to carry the information. To optimize a waveform

communications system or determine its noise performance in analytic form, mathematical models of modulation and detection have to be developed.

This chapter extends the conventional waveform communications concept to chaotic communications. A common property of chaotic modulation schemes, namely, the estimation problem that, if not prevented, corrupts the noise performance of chaotic communications systems is discussed. Then, introducing the Fourier analyzer concept, a received signal space is defined in which every received signal either deterministic, chaotic or random can be represented. Finally a step-by-step approach is given for the derivation of different detection algorithms. As examples, the derivation of coherent, averaged optimum noncoherent and autocorrelation detection algorithms and detector configurations are shown.

To show the feasibility of chaotic communications, an FM-DCSK data communications systems operating in the 2.4-GHz ISM band is implemented. The FM-DCSK transceiver is implemented in software and a universal hardware device is used to convert the signals between the RF domain and baseband.

5.1 Introduction

The radio channel transmitting the information bearing signal from the transmitter to the receiver is analog, consequently, the digital information to be transmitted has to be mapped into analog waveforms of finite duration. This approach is referred to as *waveform communications* and the modulation is the process that maps the digital information into analog waveform referred to as carrier.

Chaotic signals are wideband signals that can be generated by simple circuits in any frequency band and at arbitrary power level. If the digital information to be transmitted is mapped directly into an inherently wideband chaotic carrier then a digital chaotic communications system, considered in this chapter, is implemented. The potential application areas of chaotic communications are those where the inherently wideband characteristic of chaotic carriers is exploited.

There are two emerging applications where wideband signals have to be sent via the radio channel:

- *indoor radio communications*,
  where the radio coverage is limited by the multipath propagation and
- *frequency reuse*,
  where the radio communications is implemented in a frequency band already occupied by conventional narrowband radio links. The interference caused by the new, referred to as Ultra-WideBand (UWB) radio system, is limited by keeping the Power Spectral Density (psd) of transmitted

UWB signal below a threshold specified by the Federal Communications Commission (FCC) in the USA [6].

The digital information to be transmitted is mapped into sinusoidal waveforms in conventional digital communications. The required bandwidth is determined by the data rate and modulation scheme, the main design goal is to minimize the bandwidth required. In this sense the conventional telecommunications systems are narrowband. When the bandwidth of transmitted signal has to be increased then an additional signal, such as a pseudo-noise sequence, is used to get a Spread Spectrum (SS) system [8].

An alternative solution is the Impulse Radio (IR) approach where the digital information to be transmitted is mapped into Radio Frequency (RF) impulses [22]. The RF impulse used as carrier in UWB IR has an extremely short duration, consequently, the modulated UWB signal is an ultra-wideband signal with a very low psd in the frequency domain.

The last solution used in conventional communications is the Orthogonal Frequency-Division Multiplexing (OFDM) [23], where (i) a large number of subchannels are used, (ii) the data stream is split into parallel data substreams and (iii) each substream is sent via an independent dedicated subchannel.

Let the solutions outlined above be referred to as conventional or non-chaotic approaches. Note, the common property of non-chaotic solutions is that fixed deterministic waveforms are used as carries. Consequently, if the same symbol is transmitted repeatedly then the same waveform is radiated.

In chaotic communications the digital information to be transmitted is mapped into a continuously varying chaotic carrier. In contrast to the conventional waveform communications, the transmitted waveforms are continuously varying, even if the same symbol is transmitted repeatedly. The most significant properties of chaotic communications are as follows:

- chaotic carriers have no amplitude, frequency or phase, consequently, brand *new modulation schemes* had to be elaborated;
- transmitted waveforms are continuously varying even if the same symbol is transmitted repeatedly, consequently, the *estimation problem* appears;
- robust solution to synchronization of chaotic signals have not yet been found, consequently, the chaotic carrier cannot be recovered from the received noisy waveform. Hence, only *non-coherent detection* schemes are feasible.

Because of the special properties listed above, the well established theory of conventional digital telecommunications cannot be applied directly to chaotic communications. Starting from the well known conventional theory and keeping its terminology and notation, this chapter extends the theory of conventional waveform communications to the chaotic carriers. The results derived can be applied to any kind of waveform communications systems.

Section 5.2 extends the theory of communications with fixed waveforms

to the chaotic carriers by introducing the chaotic basis functions. It shows that in chaotic communications the basis functions are orthonormal only in mean. An undesirable consequence of this property is the estimation problem that corrupts the noise performance. A solution to the estimation problem is provided.

To derive the detector algorithms in analytical form a signal model has to be defined in which every transmitted waveform carrying a symbol defines a subspace. Two common basic properties possessed by each detector are exploited to construct the signal model, namely, (i) every detector observes the received signal corrupted by noise and interference in the radio channel only in the signalling time period and (ii) the bandwidth of observed signal is limited by a bandpass channel selection filter. Based on the outcome of this observation the detector makes an estimation for the transmitted symbol.

Section 5.3 introduces the Fourier analyzer concept where a finite-dimensional Hilbert space is defined. Its dimension is determined by the detector parameters, namely, by the product of observation time period and channel bandwidth. Any kind of received signal, either deterministic, chaotic or random, can be fully *represented* in this finite-dimensional Hilbert space, referred to as *received signal space*, without any distortion.

Each element of symbol set is fully characterized by its Fourier coefficients in the received signal space. Section 5.4 starts from this *a priori* information and gives an analytical method for the derivation of detection algorithms and, from them, the detector configurations.

Recall, chaotic carriers have no amplitude, frequency or phase, consequently the integrated circuits developed to build conventional radio transceivers cannot be used to implement chaotic communications systems, instead, a new approach is required. In Software Defined Electronics (SDE) [15], every RF bandpass signal processing algorithm is implemented in the BaseBand (BB) and a universal hardware device referred to as USRP unit is used to extract the BB information at the receiver or to reconstruct the RF bandpass signal from the BB waveform at the transmitter.

Section 5.5 uses the SDE approach to implement an FM-DCSK system in baseband. Implemented and the relevant signals are measured. The implemented 2.4-GHz FM-DCSK radio link demonstrates the feasibility of chaotic communications systems.

5.2 Generalization of Waveform Communications

Since only analog waveforms can be transmitted over a physical telecommunications channel and the data rate is determined by the system specification, the modulator of a digital telecommunications system maps the symbols to be transmitted into analog waveforms of finite duration. Note, the waveform

communications approach used here has nothing in common with the analog modulation techniques, here distinct waveforms, the elements of a *signal set*, are assigned to carry the different symbols.

To simplify the mathematical treatment of signal set let its elements be expressed as a weighted linear combination of N basis functions [8]. Consider a digital modulator where M symbols are transmitted. Each symbol m is mapped into a signal vector $\mathbf{s}_m = [s_{mn}]$ and the transmitted waveforms, i.e., the elements of signal set are defined by

$$s_m(t) = \sum_{n=1}^{N} s_{mn} g_n(t), \quad \begin{cases} 0 \le t < T \\ m = 1, 2, \ldots, M \\ n = 1, 2, \ldots, N \end{cases} \tag{5.1}$$

where $g_n(t),\ n = 1, 2, \ldots, N$ are the real-valued basis functions and $N \le M$.

Each symbol is characterized by a distinct signal vector $\mathbf{s}_m = [s_{mn}]$, $m = 1, 2, \ldots, M$ and, according to (5.1), by a distinct waveform. The signalling time period T, i.e., the duration of basis functions, is determined by the data rate. To avoid InterSymbol Interference (ISI), the value of basis functions is zero outside the signalling time interval.

During the design of a digital modulation scheme, either the elements $s_m(t)$ of signal set or the basis functions $g_n(t)$ can be chosen first. In the former approach, the basis functions are derived by the Gram-Schmidt orthogonalization procedure [8].

If fixed carriers are used then the basis functions are orthonormal

$$\int_0^T g_i(t) g_n(t) dt = \begin{cases} 1, & \text{if } i = n \\ 0, & \text{otherwise} \end{cases} \tag{5.2}$$

which means that each basis function carries unit energy and each pair of distinct basis functions are orthogonal to each other in the signalling time period $[0, T]$. Recall, the $g_n(t) = 0$ outside the signalling time period.

Signal vector $\mathbf{s}_m$ and basis functions $g_n(t)$ are *a priori* known at the receiver. This knowledge is exploited to suppress channel noise and interference at the detector. The coherent and noncoherent receivers exploit fully and partly, respectively, the *a priori* information available. The more amount of *a priori* information is exploited, the better the system performance.

The type of basis functions gives an upper bound on the *a priori* information. Based on the type of basis functions, three classes of waveform communications systems are distinguished, namely, communications with

- fixed waveforms, the conventional approach [8, 21];
- chaotic waveforms, considered here [7];
- random waveforms [3].

5.2.1 Types of basis functions

In *fixed waveform communications*, the basis functions are fixed. Consequently, every time when the same symbol is sent then the same waveform is transmitted. The basis functions and the elements of signal set are exactly known. In the built receivers the basis functions are recovered from the received signal (see the correlator receiver including a carrier recovery circuit) or stored at the receiver (see the matched filter approach) [21].

Note, the type of generator used to produce the fixed basis functions is irrelevant. The only important issue is that the basis functions are *fixed* waveforms. Even a windowed part of chaotic signal may be used as basis function in fixed waveform communications if it is stored in a memory.

In *varying waveform communications* (see chaotic communications as an example) each basis function is the actual output of a chaotic signal generator. Recall, chaotic signals are predictable only in short run because the chaotic systems have an extremely high sensitivity to the initial conditions and to the parameters of chaotic attractor [19]. The shapes of chaotic basis functions are continuously varying and different waveforms are radiated even if the same symbol is transmitted repeatedly.

Consider a chaotic waveform communications systems where the basis functions are chaotic sample functions of *finite duration*. An important feature of chaotic communications is that the transmitted signal is never periodic. On the other hand, the energy carried by chaotic sample functions is not constant and the cross-correlation of two chaotic sample functions differs from zero. Even more, the energy and cross-correlation vary from sample function to sample function. This property referred to as estimation problem is discussed in the next subsection. If unsolved, the estimation problem corrupts the noise performance of every varying waveform communications system.

In the remaining part of this chapter, the continuously varying property of chaotic basis functions is reflected by the upper index q

$$g_n^q(t), \quad q = 1, 2, \ldots \tag{5.3}$$

where q identifies the basis function transmitting the qth element of a symbol stream.

5.2.2 Estimation problem

At the receiver, the detector observes the received signal in the signalling time period, also referred to as symbol duration, T and produces the observation variable. Due to the channel imperfections (noise, multipath propagation, interference, etc.) the observation variable is a random variable characterized by its probability density function. Considering the Bit Error Rate (BER) performance, the most important parameters are the mean and the standard deviation of this distribution. The higher the variance of observation variable, the worse the BER [8]. Any effect that increases the variance of observation variable corrupts the BER performance.

Chaotic signals are not deterministic signals, consequently, they can be characterized only by their statistical parameters. To get these statistical parameters, the stochastic signal model has to be adopted to the chaotic waveforms.

The chaotic stochastic signal model has been elaborated in [10] where the ensemble of sample functions is defined as the output of a chaotic attractor starting from each possible initial condition.

Although chaotic waveforms with *infinite duration* and generated by different attractors[1] or by the same attractor but started from different initial conditions are uncorrelated and their corresponding average powers are constant, the chaotic basis functions of *finite duration* are orthonormal only in mean

$$E\left[\int_0^T g_i^q(t)g_n^q(t)dt\right] = \begin{cases} 1, & \text{if } i = n \\ 0, & \text{otherwise} \end{cases} \tag{5.4}$$

where $E[\cdot]$ denotes the expectation operator.

The integral

$$\int_0^T g_i^q(t)g_n^q(t)dt \tag{5.5}$$

gives estimates of auto- $(i = n)$ and cross- $(i \neq n)$ correlations of basis functions [4]. These estimates calculated from the sample functions of finite duration are random variables. Their variance increases the variance of observation variable and, consequently, corrupts the BER performance. To get the best BER performance, the variances of auto- and cross-correlation estimation have to be kept zero.

For $i = n$, (5.5) estimates the energy of ith basis function. Equation (5.5) shows that if the chaotic signals are directly used as basis functions then the energy used to transmit one symbol is not constant but varies from symbol to symbol. This property is called autocorrelation estimation problem. The mean and standard deviation of estimation of $\int_0^T [g_n^q(t)]^2 dt$ versus the estimation time, i.e., the symbol duration, are plotted in Fig. 5.1(a), where the chaotic basis function was generated by a third-order analog phase locked loop (APLL) [17].

The effect of cross-correlation estimation problem is shown in Fig. 5.1(b), where the basis functions were generated by the same chaotic APLL but started from different initial conditions. Due to the cross-correlation estimation problem an interference among the different basis functions that corrupts the BER performance appears.

The standard deviations of both estimates are inversely proportional to the product of estimation time and the equivalent statistical bandwidth of chaotic basis functions [10]. The former and latter are equal to the symbol duration and RF bandwidth of chaotic basis functions, respectively.

[1] In this respect, attractors described by the same mathematical model but having different parameters are considered as different attractors.

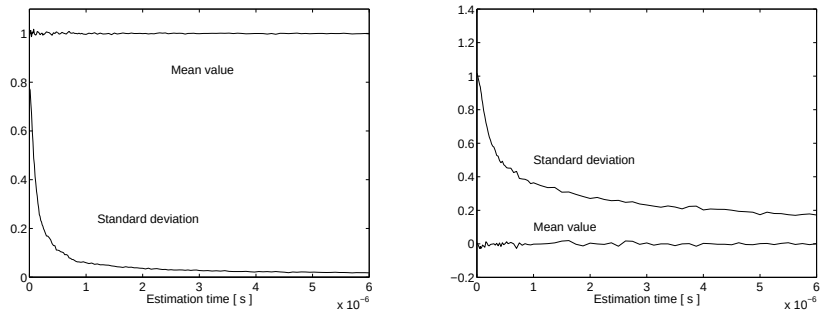

(a) (b)

FIGURE 5.1
The mean and standard deviation of estimation versus the estimation time: (a) Autocorrelation and (b) cross-correlation estimation problems.

The estimation problem is present in every modulation scheme where the basis functions are *orthonormal only in mean*. It appears in both the chaotic and random modulation techniques. To solve the estimation problem there is no need to fix the shape of basis function, it is enough to satisfy the condition (5.2) of orthonormality for each sample of basis functions.

5.2.3 Chaotic modulation schemes

Digital modulation using chaotic basis functions and coherent receiver was first introduced in 1992 [20] and referred to as Chaos Shift Keying (CSK) [5]. A coherent receiver needs a carrier recovery circuit being robust against the channel imperfections such as noise, interference, multipath propagation, etc. A lot of research effort has been done to develop a synchronization technique for chaotic carrier recovery but these efforts failed. Chaotic synchronization is not feasible because of its high sensitivity to channel imperfections.

The first robust noncoherent modulation technique referred to as Differential Chaos Shift Keying (DCSK) [18] was introduced in 1996, and later optimized as Frequency-Modulated DCSK (FM-DCSK) [14].

5.2.3.1 Antipodal binary CSK: Modulation with one basis function

Let E_b denote the energy used to transmit one bit information. In antipodal Binary CSK (BCSK), (i) only one chaotic basis function $g_1^q(t)$ is used, and (ii) bits "1" and "0" are represented by $s_{11} = \sqrt{E_b}$ and $s_{21} = -\sqrt{E_b}$, respectively. According to (5.1), the modulated waveforms, i.e., the elements of signal set, are

$$s_m^q(t) = \pm\sqrt{E_b}\, g_1^q(t), \quad m = 1, 2. \tag{5.6}$$

To show the effect of estimation problem, the noise performance of a BCSK system implemented with varying and constant E_b has been evaluated [12]. Because only one chaotic sample function is used in BCSK, only the autocorrelation estimation problem is present. Figure 5.2 shows the manifestation of estimation problem, dash-dotted and solid curves give the noise performances versus the energy per bit-to-noise spectral density ratio E_b/N_0 for the cases when the energy of basis function is varying or is kept constant, respectively. As expected, the estimation problem increases the variance of observation variable and, consequently, corrupts the noise performance.

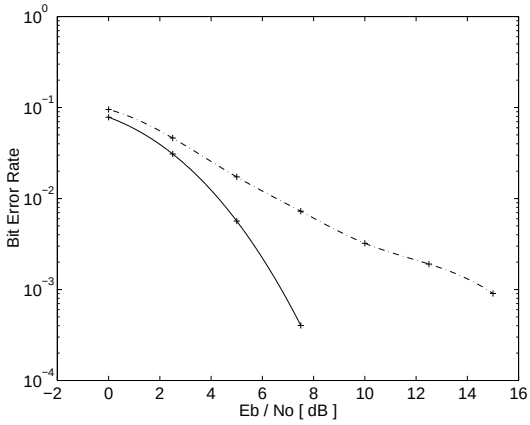

FIGURE 5.2
The noise performance of BCSK for varying (dash-dotted curve) and constant (solid curve) E_b.

5.2.3.2 FM-DCSK: Modulation with two basis function

In binary FM-DCSK, the two elements of signal set representing bits "1" and "0," respectively, are defined by

$$s_1^q(t) = \sqrt{E_b}\, g_1^q(t) \quad \text{and} \quad s_2^q(t) = \sqrt{E_b}\, g_2^q(t) \tag{5.7}$$

where the two basis functions $g_1^q(t)$ and $g_2^q(t)$ are constructed from a frequency-modulated chaotic waveform $c^q(t)$ and the first two Walsh functions [13]

$$\begin{aligned} g_1^q(t) &= \begin{cases} c^q(t), & 0 \le t < T/2 \\ c^q(t - T/2), & T/2 \le t < T, \end{cases} \\ g_2^q(t) &= \begin{cases} c^q(t), & 0 \le t < T/2 \\ -c^q(t - T/2), & T/2 \le t < T\,. \end{cases} \end{aligned} \tag{5.8}$$

Equations (5.7) and (5.8) show that FM-DCSK maps every bit to be transmitted into two consecutive waveforms of duration $T/2$. The first one serves as a reference while the second one carries the information. For bit "1," the information bearing waveform is identical to the reference one while for bit "0," it is an inverted copy of the reference waveform. Note, FM-DCSK belongs to the class of transmitted reference systems. FM-DCSK is a noncoherent modulation scheme that can be demodulated without carrier recovery.

To avoid the autocorrelation estimation problem, the frequency-modulated chaotic waveform $c^q(t)$ in (5.8) is generated by an FM modulator. The chaotic signal is fed into the FM modulator input, $c^q(t)$ appears at the modulator output, and the bandwidth of $c^q(t)$ is set by the parameters of chaotic attractors and FM modulator [9]. Value of $c^q(t)$ is zero outside the time interval $[0, T/2]$. Note, the frequency-modulated chaotic waveform $c^q(t)$ is continuously varying, but because of the FM modulator, it is a constant envelope signal. Consequently, its energy is constant and $\int_0^{T/2}[c^q(t)]^2 dt = 1/2$.

In FM-DCSK both the autocorrelation and cross-correlation estimation problems are avoided. The constant energy and orthogonality of basis functions are assured by FM and the first two Walsh functions, respectively. The FM-DCSK basis functions are always orthonormal regardless of the shape of continuously varying chaotic signals.

5.3 Signal Model for Detection

In digital communications, the elements of signal set carrying the symbols pass through a telecommunications channel in which they are corrupted by noise and interference, and may suffer from distortion and multipath effect. Observing the corrupted and distorted received analog waveform in the time interval of symbol duration, the detector must decide which symbol has been most likely transmitted.

According to (5.1), the elements of signal set are constructed from the basis functions and signal vector. This *a priori* information is exploited to perform the detection and suppress channel noise and interference at the receiver.

This section defines a *finite-dimensional discrete* Hilbert space referred to as *received signal space* in which each signal passing through the channel selection filter, either deterministic or random, is represented by their Fourier coefficients. The *a priori* information available is also quantified by the Fourier coefficients. These coefficients will be used in Sec. 5.4 to derive the different detection algorithms.

5.3.1 General block diagram of a receiver

Consider an Additive White Gaussian Noise (AWGN) channel [8] and let N_0 denote the psd of channel noise. Symbol m is transmitted by sending the analog waveform $s_m^q(t)$ to the receiver via the analog radio channel where it is corrupted by Gaussian white noise or channel interference $n(t)$ as shown in Fig. 5.3. The received signal $r_m^q(t) = s_m^q(t) + n(t)$ is bandlimited by the bandpass channel (selection) filter having an RF bandwidth of $2B$. The noisy filtered signal $\tilde{s}_m^q(t) + \tilde{n}(t)$ is observed by the detector in the symbol duration T to generate the *observation variable* $\mathbf{z}_m$, a random quantity.

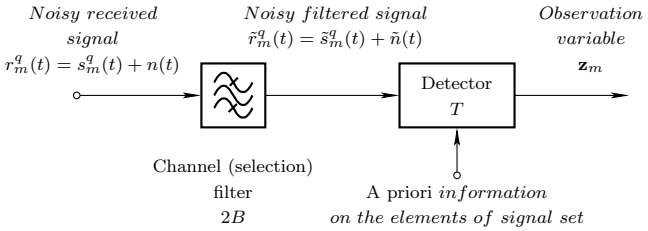

FIGURE 5.3
General block diagram of a digital waveform communications receiver.

The (i) decision time instants, (ii) bit duration T and (iii) RF bandwidth $2B$ of transmitted signal $s_m^q(t)$ are always known at the receiver.

5.3.2 Fourier analyzer concept

Consider the noise-free case first and assume that the channel filter passes the transmitted signal without any distortion, i.e., $\tilde{r}_m^q(t) = \tilde{s}_m^q(t) = s_m^q(t)$. To get a *discrete* Hilbert space in the frequency domain, a periodic signal has to be constructed in the time domain from the received signal.

Because the detector observes the received signal only in the time interval $[0, T)$, $s_m^q(t)$ can be substituted by a periodic signal

$$s_{T,m}^q(t) = \begin{cases} s_m^q(t), & \text{for } 0 \le t < T \\ s_m^q(t - CT), & \text{otherwise} \end{cases} \tag{5.9}$$

where C is an arbitrary nonzero integer. The introduction of the periodic signal in (5.9) does not cause any distortion since the two signals, the received one and its periodic equivalent, *coincide* each other in the observation time period, i.e., the symbol duration.

In the Fourier analyzer concept [16], the received signal space is a Hilbert space spanned by the harmonically related sinusoidal basis functions

$$\cos\left(k\frac{2\pi}{T}t\right) \quad \text{and} \quad \sin\left(k\frac{2\pi}{T}t\right)$$

where the frequencies $k/T,\ k = 1, 2, \cdots$ of this Fourier base are determined by the observation time period.

The detector projects the filtered received waveform $\tilde{r}_m^q(t) = s_m^q(t)$ in $0 \le t < T$ into the Hilbert space and returns its Fourier coefficients

$$\begin{aligned} a_{mk}^q &= \frac{2}{T}\int_0^T s_m^q(t)\cos\left(k\frac{2\pi}{T}t\right)dt, \\ b_{mk}^q &= \frac{2}{T}\int_0^T s_m^q(t)\sin\left(k\frac{2\pi}{T}t\right)dt\,. \end{aligned} \tag{5.10}$$

When the channel noise and interference are also considered in the receiver model depicted in Fig. 5.3 then the detector observes $\tilde{r}_m^q(t) = \tilde{s}_m^q(t) + \tilde{n}(t)$ and (5.10) gives only *estimates*, denoted by hats, of the Fourier coefficients

$$\begin{aligned} \hat{a}_{mk}^q &= \frac{2}{T}\int_0^T \tilde{r}_m^q(t)\cos\left(k\frac{2\pi}{T}t\right)dt, \\ \hat{b}_{mk}^q &= \frac{2}{T}\int_0^T \tilde{r}_m^q(t)\sin\left(k\frac{2\pi}{T}t\right)dt\,. \end{aligned} \tag{5.11}$$

If the Signal-to-Noise Ratio (SNR) is high enough then we obtain

$$\tilde{r}_{T,m}^q(t) = \sum_{k=K_1}^{K_2}\left[\hat{a}_{mk}^q\cos\left(k\frac{2\pi}{T}t\right) + \hat{b}_{mk}^q\sin\left(k\frac{2\pi}{T}t\right)\right] \approx s_{T,m}^q(t) \tag{5.12}$$

where, as will be shown below, the constants K_1 and K_2 are determined by the parameters of channel filter.

The periodicity introduced in (5.9) gives a *discrete* received signal space. Now the dimension of this space has to be found.

The channel filter, an ideal bandpass filter, limits the bandwidth of the signal observed by the detector in $2B$. Figure 5.4 shows the location of Fourier series coefficients of $\tilde{r}_{T,m}^q(t)$ by arrows in the frequency domain. The channel filter suppresses each spectral component lying outside the frequency range

$$(2K_1 - 1)/2T \le f \le (2K_2 + 1)/2T$$

where K_1 and K_2 are determined by the center frequency f_0 and bandwidth $2B$ of channel filter

$$K_1 = \frac{2(f_0 - B)T + 1}{2} \quad \text{and} \quad K_2 = \frac{2(f_0 + B)T - 1}{2}\,. \tag{5.13}$$

By definition, the signal dimension gives the number of harmonically related sinusoidal basis functions along which the receiver collects information on the received signal

$$S_D = 2(K_2 - K_1 + 1) = 4BT\,. \tag{5.14}$$

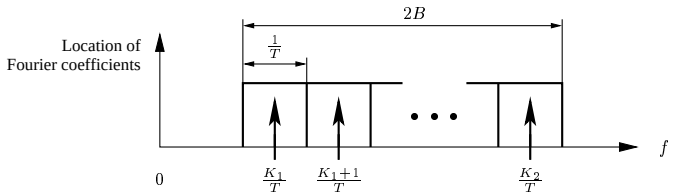

FIGURE 5.4
Location of Fourier series coefficients of $\tilde{r}^q_{T,m}(t)$ in the frequency domain.

In other words, the signal dimension S_D gives the dimension of Hilbert space spanned by the Fourier base which is required to represent *any signal* appearing at the detector input *in the observation time interval*. Note, the dimension of received signal space does not depend on the center frequency of telecommunications channel, it is given by the *always known* receiver parameters, namely, by the product of observation time period T and receiver bandwidth $2B$.

5.3.3 Quantifying *"a priori"* information

After channel filtering, the detector projects the received waveform into the received signal space and returns its Fourier coefficients. These Fourier coefficients are compared against the *a priori* information to get the observation variable.

To make the comparison possible, the *a priori* information also has to be expressed in the form of Fourier coefficients. They are obtained by projecting the basis functions $g^q_n(t),\ n = 1, 2, \cdots, N$ into the received signal space

$$\begin{aligned} \alpha^q_{nk} &= \frac{2}{T}\int_0^T g^q_n(t)\cos\left(k\frac{2\pi}{T}t\right)dt \\ \beta^q_{nk} &= \frac{2}{T}\int_0^T g^q_n(t)\sin\left(k\frac{2\pi}{T}t\right)dt \end{aligned} \tag{5.15}$$

These Fourier coefficients quantify the *a priori* information.

5.4 Derivation of Detection Algorithms

The Fourier coefficients (5.11) of received signal are determined and compared against those (5.15) of the *a priori* known basis functions. The tool of comparison is the inner product. The result, referred to as *observation variable*, is used to perform the decision.

This section focuses on the derivation of detection algorithms, consequently, only the transmission of a single isolated symbol is considered. Interference has to be prevented by forming a Nyquist channel as done in conventional telecommunications systems [8].

The type of detector depends on the extent to which the *a priori* information carried by α_{nk}^q and β_{nk}^q in (5.15) is exploited during the derivation of detection algorithm. As the most important examples, three detection algorithms are derived here

- *coherent detection*, where all *a priori* information carried by α_{nk} and β_{nk} are exploited;
- *optimum noncoherent detection*, where only the harmonic amplitudes $\gamma_{nk}^q = \sqrt{\left(\alpha_{nk}^q\right)^2 + \left(\beta_{nk}^q\right)^2}$ of basis functions are considered;
- *autocorrelation detection*, where only the separation of spectra of signals carrying bits "1" and "0" are exploited. Here the minimum amount of *a priori* information is exploited, consequently, this approach gives the worse BER performance.

5.4.1 Coherent detection algorithm

Coherent detector fully exploits the *a priori* information available, consequently, it offers the best BER performance.

Consider an antipodal BCSK modulation where the elements of signal set are given by (5.6). The detector projects the noisy filtered received waveform $\tilde{r}_m^q(t)$ into the received signal space and returns a vector of estimates of its Fourier coefficients

$$\left(\hat{\mathbf{r}}_{\mathbf{m}}{}^q\right)' = \left(\hat{a}_{mK_1}^q \; \hat{b}_{mK_1}^q \; \cdots \; \hat{a}_{mk}^q \; \hat{b}_{mk}^q \; \cdots \; \hat{a}_{mK_2}^q \; \hat{b}_{mK_2}^q\right) \tag{5.16}$$

where $\hat{a}_{m,k}^q$ and $\hat{b}_{m,k}^q$ are given by (5.11), $K_1 \leq k \leq K_2$ are obtained from (5.13) and the prime character $'$ denotes the transpose of a vector.

From (5.15), a vector of Fourier coefficients of *a priori* information is obtained as

$$\left(\mathbf{g_1}{}^q\right)' = \left(\alpha_{1K_1}^q \; \beta_{1K_1}^q \; \cdots \; \alpha_{1k}^q \; \beta_{1k}^q \; \cdots \; \alpha_{1K_2}^q \; \beta_{1K_2}^q\right) . \tag{5.17}$$

The signal space is a Hilbert space, consequently, the closeness of the two Fourier coefficient vectors defined by (5.16) and (5.17) is expressed by their inner product as

$$C_{\hat{\mathbf{r}}\mathbf{m}\mathbf{g_1}}^q = \left(\hat{\mathbf{r}}_{\mathbf{m}}{}^q\right)' \cdot \mathbf{g_1}{}^q = \sum_{k=K_1}^{K_2} \left(\hat{a}_{mk}^q \, \alpha_{1k}^q + \hat{b}_{mk}^q \, \beta_{1k}^q\right) \tag{5.18}$$

The observation variable is obtained from the inner product. Substituting

(5.11) into (5.18) and exchanging the order of the sum and integration, the observation variable is obtained as

$$z_{m1}^{q} = \frac{T}{2} C_{\hat{\mathbf{r}}\mathbf{m}\mathbf{g_1}}^{q} = \int_0^T \tilde{r}_m^q(t) \sum_{k=K_1}^{K_2} \left[\alpha_{1k}^q \cos\left(k\frac{2\pi}{T}t\right) + \beta_{1k}^q \sin\left(k\frac{2\pi}{T}t\right) \right] dt$$

Recognizing that the sum on the RHS is the Fourier series representation of the basis function $g_1(t)$ in the observation time period, the detection algorithm for the coherent receiver is obtained as

$$z_{m1}^{q} = \int_0^T \tilde{r}_m^q(t) g_1^q(t) dt \tag{5.19}$$

The block diagram of coherent detector constructed from (5.19) is depicted in Fig. 5.5. The decision circuit is a comparator with zero threshold and it generates the estimate $\hat{b}_m$ of transmitted bit.

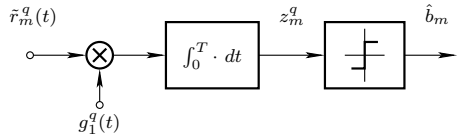

FIGURE 5.5
Block diagram of a coherent detector.

Fixed waveforms are used in conventional communications, consequently, in that case q has to be suppressed in (5.19) and in Fig. 5.5. The basis function and decision time instants are recovered from the received signal by the carrier and clock recovery circuits, respectively. Note, the block diagram depicted in Fig. 5.5 is identical with the coherent correlation receiver known from the literature [8].

Coherent chaos based communications systems are not feasible because a robust solution to the recovery of a chaotic basis function from the received signal has not yet been found.

5.4.2 Averaged optimum noncoherent detection algorithm

To get the averaged optimum noncoherent detector, the harmonic form of Fourier series representation has to be used in (5.12)

$$\tilde{r}_{T,m}^{q}(t) = \sum_{k=K_1}^{K_2} A_k^q \cos\left(k\frac{2\pi}{T}t - \theta_k^q\right)$$

where each harmonic Fourier series component is defined by its harmonic amplitude and phase angle

$$\hat{A}_{mk}^{q} = \sqrt{\left(\hat{a}_{mk}^{q}\right)^2 + \left(\hat{b}_{mk}^{q}\right)^2} \quad \text{and} \quad \hat{\theta}_{mk}^{q} = \tan^{-1}\left(\hat{b}_{mk}^{q}/\hat{a}_{mk}^{q}\right), \tag{5.20}$$

respectively. In the optimum noncoherent approach, the phase information is neglected and only the harmonic amplitudes are used to derive the detection algorithm.

Assume that the recovery of chaotic basis functions is not feasible, consequently, a noncoherent detection algorithm has to be developed. Because the basis functions are continuously varying, only the *averages* of harmonic amplitudes of basis functions are available

$$\overline{\gamma_{nk}^{q}} = \mathrm{E}\left[\gamma_{nk}^{q}\right] = \mathrm{E}\left[\sqrt{(\alpha_{nk}^{q})^2 + (\beta_{nk}^{q})^2}\right] \tag{5.21}$$

where E[·] denotes averaging over q and the averaged harmonic amplitudes $\overline{\gamma_{nk}^{q}}$ can be determined from the spectrum of chaotic basis function $g_n(t)$ [9].

Both the neglected phase information and averaging reduce the amount of exploited *a priori* information, consequently, the noise performance of averaged optimum noncoherent detector will be worse than that of the coherent one.

Projecting the received filtered waveform $\tilde{r}_m^q(t)$ into the received signal space, a vector of estimates of its harmonic amplitudes (5.20) is obtained as

$$(\hat{\mathbf{r}}\mathbf{m}^{q})' = \left(\hat{A}_{mK_1}^{q} \;\cdots\; \hat{A}_{mk}^{q} \;\cdots\; \hat{A}_{mK_2}^{q}\right). \tag{5.22}$$

The *exploited a priori* information is expressed by a vector of averaged harmonic amplitudes (5.21) of basis functions

$$(\mathbf{g}\mathbf{n}^{q})' = \left(\overline{\gamma_{nK_1}^{q}} \;\cdots\; \overline{\gamma_{nk}^{q}} \;\cdots\; \overline{\gamma_{nK_2}^{q}}\right). \tag{5.23}$$

The observation variable is the weighted inner product of (5.22) and (5.23)

$$z_{mn}^{q} = \frac{T}{2} C_{\hat{\mathbf{r}}\mathbf{m}\mathbf{g}\mathbf{n}}^{q} = (\hat{\mathbf{r}}\mathbf{m}^{q})' \cdot \mathbf{g}\mathbf{n}^{q} = \frac{T}{2} \sum_{k=K_1}^{K_2} \hat{A}_{mk}^{q}\, \overline{\gamma_{nk}^{q}} \tag{5.24}$$

Substituting (5.11) into (5.20), then substituting (5.20) and (5.21) into (5.24), the observation variable is obtained as

$$\begin{aligned} z_{mn}^{q} = & \sum_{k=K_1}^{K_2} \overline{\gamma_{nk}^{q}} \\ & \times \sqrt{\left[\int_0^T \tilde{r}_m^{q}(t) \cos\left(k\frac{2\pi}{T}t\right) dt\right]^2 + \left[\int_0^T \tilde{r}_m^{q}(t) \sin\left(k\frac{2\pi}{T}t\right) dt\right]^2} \end{aligned} \tag{5.25}$$

Recall, the exploited *a priori* information is represented by $\overline{\gamma_{nk}^q}$, i.e., by the *averages of harmonic amplitudes* of chaotic basis functions.

Consider a binary modulation scheme where two basis functions are used and the two elements of signal set are defined by (5.7). The observation variable (5.25) has to be determined for both basis functions and the decision is done in favor of bit "1" if

$$z_{11}^q > z_{22}^q \qquad \text{or} \qquad z_{11}^q - z_{22}^q > 0\,. \tag{5.26}$$

The block diagram of binary averaged optimum noncoherent detector constructed from (5.25) and (5.26), is depicted in Fig. 5.6.

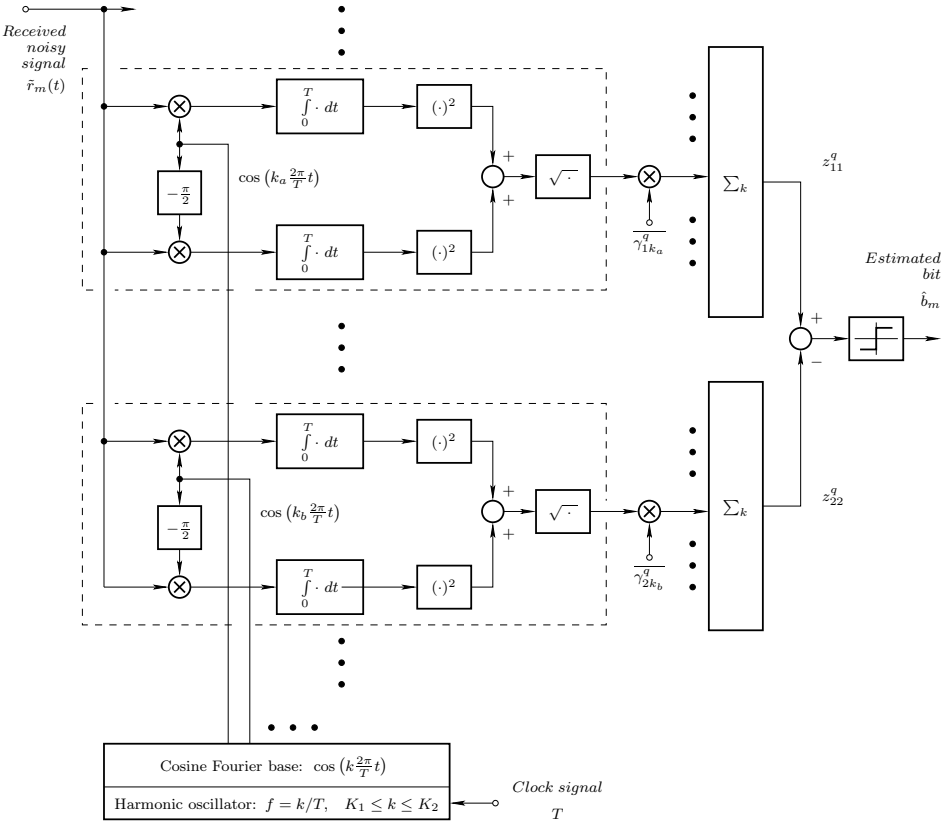

FIGURE 5.6
Block diagram of an averaged optimum noncoherent detector.

The block diagram shown in Fig. 5.6 is also valid for fixed waveform communications. Consider a binary FSK modulation with signalling frequencies $f_1 = k_a/T$ and $f_2 = k_b/T$. In fixed waveform communications q has to be suppressed and $\overline{\gamma_{nk}^q} = \sqrt{2/T}$. The circuits included in dashed boxes in Fig. 5.6 are

the quadrature equivalents of *noncoherent matched filters* [8]. Each of them is matched to one of signalling frequencies, the upper and lower ones to f_1 and f_2, respectively. Note, the block diagram depicted in Fig. 5.6 is the generalization of the optimum noncoherent receiver concept to the varying waveform communications.

5.4.3 Autocorrelation detection algorithm

Binary DCSK/FM-DCSK uses two basis functions (5.8), the orthogonality of $g_1^q(t)$ and $g_2^q(t)$ is assured by the first two Walsh functions. The spectra of $g_1^q(t)$ and $g_2^q(t)$ are separated in the frequency domain, this separation is exploited to derive the autocorrelation detection algorithm. Because the least amount of *a priori* information is exploited in autocorrelation detector, it offers the worst noise performance. To find the separation of spectra in frequency domain, the Fourier coefficients of the two basis functions have to be determined.

Let $T_C = T/2$ denote the chip duration. The Fourier series coefficients of $g_{T,1}^q(t)$ are obtained from (5.8) as

$$\alpha_{1k}^q = \frac{2}{T}\int_0^T g_{T,1}^q(t)\cos(k\frac{2\pi}{T}t)dt = \frac{1}{T_C}\int_0^{T_C} c^q(t)\cos(k\frac{2\pi}{T}t)dt + \frac{1}{T_C}\int_{T_C}^{T} c^q(t-T_C)\cos\left[k\frac{2\pi}{T}(t-T_C+T_C)\right]dt$$

where $k\frac{2\pi}{T}(T_C - T_C)$ has been added to the argument of second cosine function on the RHS. By introducing a new variable $\hat{t} = t - T_C$ in the second term of the RHS and using the trigonometric identity $\cos(\alpha+\beta) = \cos(\alpha)\cos(\beta) - \sin(\alpha)\sin(\beta)$ we get

$$\alpha_{1k}^q = \frac{1}{T_C}\int_0^{T_C} c^q(t)\cos(k\frac{2\pi}{T}t)dt + \frac{\cos(k\pi)}{T_C}\int_0^{T_C} c^q(\hat{t})\cos(k\frac{2\pi}{T}\hat{t})d\hat{t} - \frac{\sin(k\pi)}{T_C}\int_0^{T_C} c^q(\hat{t})\sin(k\frac{2\pi}{T}\hat{t})d\hat{t}.$$

Since $\sin(k\pi) = 0$ and $\cos(k\pi) = (-1)^k,\ k = 1, 2, \cdots$, we obtain

$$\alpha_{1k}^q = \begin{cases} \frac{2}{T_C}\int\limits_0^{T_C} c^q(t)\cos(k\frac{2\pi}{T}t)dt, & \text{for even } k \\ 0, & \text{for odd } k\,. \end{cases} \tag{5.27}$$

In a similar manner we get

$$\beta_{1k}^q = \begin{cases} \frac{2}{T_C}\int\limits_0^{T_C} c^q(t)\sin(k\frac{2\pi}{T}t)dt, & \text{for even } k \\ 0, & \text{for odd } k\,. \end{cases} \tag{5.28}$$

The following essential conclusions may be drawn from (5.27) and (5.28):

(i) the fundamental period of the Fourier series representation of $g_1(t)$ is equal to the observation time period T, (ii) the spectrum of the first basis function $g_1(t)$ has only *even* harmonic components.

Applying the same approach to the second base function, the Fourier coefficients of $g_{T,2}(t)$ are obtained as

$$\alpha_{2k}^q = \begin{cases} 0, & \text{for even } k \\ \frac{2}{T_C} \int\limits_0^{T_C} c^q(t) \cos(k\frac{2\pi}{T}t)dt, & \text{for odd } k \end{cases} \tag{5.29}$$

and

$$\beta_{2k}^q = \begin{cases} 0, & \text{for even } k \\ \frac{2}{T_C} \int\limits_0^{T_C} c^q(t) \sin(k\frac{2\pi}{T}t)dt, & \text{for odd } k\,. \end{cases} \tag{5.30}$$

Note, the spectrum of second basis function $g_2(t)$ has only *odd* harmonic components.

To verify (5.27)–(5.30), the spectrum of a modulated FM-DCSK signal with bit duration $T = 2$ μs and $2B = 17$ MHz was determined by computer simulation. The center frequency of modulated FM-DCSK signal was 2.4 GHz. Figure 5.7(a) and 5.7(b) show the spectrum when a pure bit "1" sequence and a pure bit "0" sequence, respectively, were generated. As predicted, the spectra of two FM-DCSK signals are fully separated in the frequency domain, although they overlap each other. The two spectra may be interpreted as the teeth of two combs fitted into one another.

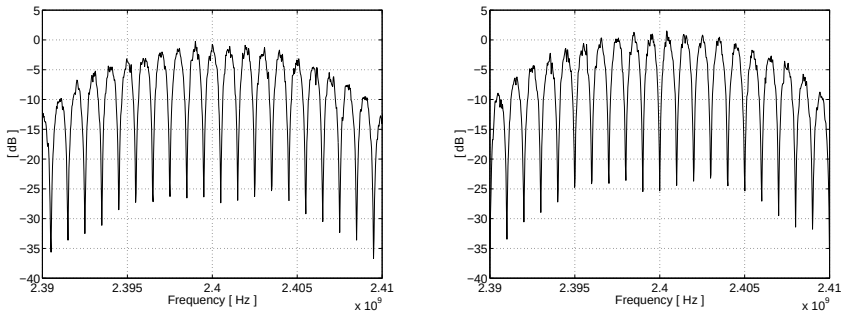

(a) (b)

FIGURE 5.7
Spectrum of FM-DCSK signal with $1/T = 500$ kHz when (a) a pure bit "1" and (b) a pure bit "0" sequence is transmitted.

The autocorrelation detector is a *noncoherent* detector which exploits *only the separation* of spectra of two basis functions in the frequency domain. Let

$\overline{\gamma_{nk}^q} = 1$ be set in (5.25) for that subspace in which the received energy has to be determined. Then (5.25) can be rearranged as

$$\frac{2}{T}\left(z_{mn}^q\right)^2 = \frac{T}{2}\sum_{k=K_1}^{K_2}\left(\left[\frac{2}{T}\int_0^T \tilde{r}_m^q(t)\cos\left(k\frac{2\pi}{T}t\right)dt\right]^2 + \left[\frac{2}{T}\int_0^T \tilde{r}_m^q(t)\sin\left(k\frac{2\pi}{T}t\right)dt\right]^2\right). \tag{5.31}$$

Substituting (5.11) into (5.31) and applying the Parseval theorem, the received energy measured in the mth subspace is obtained as

$$\frac{2}{T}\left(z_{mn}^q\right)^2 = \frac{T}{2}\sum_{k=K_1}^{K_2}\left[\left(\hat{a}_{mk}^q\right)^2 + \left(\hat{b}_{mk}^q\right)^2\right] \equiv E_m^q\,. \tag{5.32}$$

The FM-DCSK autocorrelation detector determines the received energy in the *"even"* and *"odd"* subspaces defined by (5.27)–(5.28) and (5.29)–(5.30), respectively, and makes the decision in favor of subspace, and bit, that collects the larger amount of energy.

Let the energy measured in the even subspace calculated first. The even subspace is defined by the first basis functions and is identified by $m = 1$. According to (5.27)–(5.28), the energy components have to be collected along the even harmonics in the received signal space, consequently,

$$\overline{\gamma_{1k}^q} = \begin{cases} 1, & \text{for even } k \\ 0, & \text{for odd } k \end{cases}$$

has to be submitted into (5.25).

Consider the FM-DCSK modulation scheme here. The energy per bit is kept constant by FM in FM-DCSK, consequently, the upper index q is suppressed in the remaining part of this section. The energy measured in the even subspace is obtained from (5.31) and (5.32) as

$$E_1 = \frac{T_C}{4}\sum_{\hat{k}=\hat{K}_1}^{\hat{K}_2}\left(\left[\frac{2}{T_C}\int_0^{T_C}\tilde{r}_m(t)\cos(\hat{k}\frac{2\pi}{T_C}t)dt + \frac{2}{T_C}\int_{T_C}^{T}\tilde{r}_m(t)\cos(\hat{k}\frac{2\pi}{T_C}t)dt\right]^2 + \left[\frac{2}{T_C}\int_0^{T_C}\tilde{r}_m(t)\sin(\hat{k}\frac{2\pi}{T_C}t)dt + \frac{2}{T_C}\int_{T_C}^{T}\tilde{r}_m(t)\sin(\hat{k}\frac{2\pi}{T_C}t)dt\right]^2\right) \tag{5.33}$$

where $T_C = T/2$ has been substituted and each integral in (5.31) has been decomposed into two parts, first the reference then the information bearing parts of received signal are integrated. Since k is even for bit "1," $\hat{k}$ is a positive integer.

To have only one observation time period, i.e., the simplest detector configuration, each integral in (5.33) should be evaluated from T_C to T.

Let a new variable $\hat{t}=t+T_C$ be introduced. Since $\cos[\hat{k}\frac{2\pi}{T_C}(\hat{t}-T_C)]$ $=\cos(\hat{k}\frac{2\pi}{T_C}\hat{t}-2\pi\hat{k})=\cos(\hat{k}\frac{2\pi}{T_C}\hat{t})$, the first term in (5.33) becomes

$$\frac{2}{T_C}\int_0^{T_C}\tilde{r}_m(t)\cos(\hat{k}\frac{2\pi}{T_C}t)dt=\frac{2}{T_C}\int_{T_C}^{T}\tilde{r}_m(\hat{t}-T_C)\cos(\hat{k}\frac{2\pi}{T_C}\hat{t})d\hat{t}\,. \tag{5.34}$$

In a similar manner, the third term in (5.33) may be written as

$$\frac{2}{T_C}\int_0^{T_C}\tilde{r}_m(t)\sin(\hat{k}\frac{2\pi}{T_C}t)dt=\frac{2}{T_C}\int_{T_C}^{T}\tilde{r}_m(\hat{t}-T_C)\sin(\hat{k}\frac{2\pi}{T_C}\hat{t})d\hat{t}\,. \tag{5.35}$$

Substituting (5.34) and (5.35) into (5.33) and introducing $t=\hat{t}$ as a new variable we get

$$E_1=\frac{T_C}{4}\sum_{\hat{k}=\hat{K}_1}^{\hat{K}_2}\left(\left[\frac{2}{T_C}\int_{T_C}^{T}\tilde{r}_m(t-T_C)\cos(\hat{k}\frac{2\pi}{T_C}t)dt+\frac{2}{T_C}\int_{T_C}^{T}\tilde{r}_m(t)\cos(\hat{k}\frac{2\pi}{T_C}t)dt\right]^2\right.$$
$$\left.+\left[\frac{2}{T_C}\int_{T_C}^{T}\tilde{r}_m(t-T_C)\sin(\hat{k}\frac{2\pi}{T_C}t)dt+\frac{2}{T_C}\int_{T_C}^{T}\tilde{r}_m(t)\sin(\hat{k}\frac{2\pi}{T_C}t)dt\right]^2\right). \tag{5.36}$$

Recall, the received signal space is discrete Hilbert space where every signal is represented by its periodic equivalent. The FM-DCSK signal is constructed from two chips, the first and second ones are referred to as reference and information bearing chips, respectively. These two chips are identified by "**R**" and "**I**" in Fig. 5.8(a).

The expression in the bracket on the RHS of (5.36) can be interpreted as follows: the second and forth terms give the Fourier series coefficients of the information bearing chip, while the first and third terms define those of the *delayed* reference chip. These two chips are depicted in Fig. 5.8(b).

Figure 5.8(b) shows the delayed reference and information bearing chips represented in the even subspace, a discrete Hilbert space. Similarly to (5.9), the two chips are substituted by periodic ones where the two chips and their periodic equivalents are identical in the time period of $T_c\le t<T$, in the time interval in which the integrals in (5.36) are evaluated. Note, the period time is equal to T_C and not T in the even subspace. To avoid confusion, the reference and information bearing chips are plotted only in the time period of $T_c\le t<T$ in Fig. 5.8(b) and the periodicity of signals is marked by dots.

Let $\hat{a}_{1\hat{k}}^{R,del}$ and $\hat{b}_{1\hat{k}}^{R,del}$ denote the estimated Fourier series coefficients of the delayed reference $\tilde{r}_{T_C,m}^{R}(t-T_C)$ and let $\hat{a}_{1\hat{k}}^{I}$ and $\hat{b}_{1\hat{k}}^{I}$ define those of the

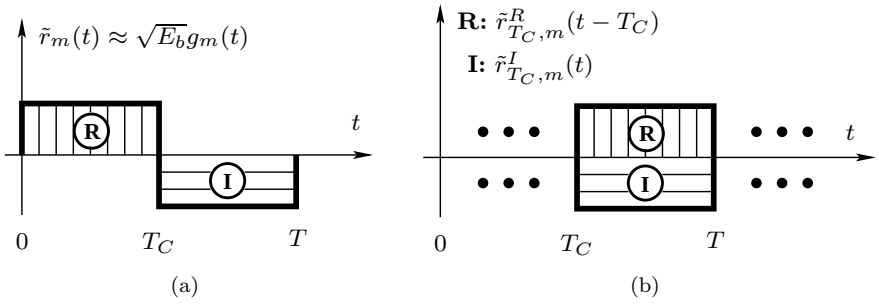

FIGURE 5.8
Structure of received FM-DCSK signal: (a) in its original form and (b) its equivalent represented in the even discrete subspace after time shifting.

information bearing $\tilde{r}^I_{T_C,m}(t)$ chips. Then from (5.36) we obtain

$$E_1 = \frac{T_C}{4} \sum_{\hat{k}=\hat{K}_1}^{\hat{K}_2} \left[\left(\hat{a}^{R,del}_{1\hat{k}} + \hat{a}^I_{1\hat{k}} \right)^2 + \left(\hat{b}^{R,del}_{1\hat{k}} + \hat{b}^I_{1\hat{k}} \right)^2 \right] . \tag{5.37}$$

The signals $\tilde{r}^R_{T_C,m}(t - T_C)$ and $\tilde{r}^I_{T_C,m}(t)$ are periodic signals with a period time of T_C. The Parseval's identity expresses the relationship between the average power of a periodic signal and its Fourier series coefficients. The received signal is an RF bandpass signal, consequently, it has a zero DC component. Exploiting the Parseval's identity, (5.37) can be interpreted as follows:

- RHS of (5.37) shows that the sum of two RF bandpass periodic signals with the same periodicity T_C has to be considered in the time domain;
- the two bandpass signals are the delayed reference and the information bearing chips of received signal as depicted in Fig. 5.8(b).

Based on these observations, (5.37) can be reformulated as

$$E_1 = \frac{1}{2} \int_{T_C}^{T} \left[\tilde{r}^R_{T_C,m}(t - T_C) + \tilde{r}^I_{T_C,m}(t) \right]^2 dt .$$

The limits of integration show that the detector observes the received signal only in the time period of $T_c \leq t < T$. Note, the delayed reference and the information bearing chips are equal to $\tilde{r}^R_{T_C,m}(t - T_C)$ and $\tilde{r}^I_{T_C,m}(t)$, respectively, in this time interval. Hence, the energy received in the even subspace is obtained as

$$E_1 = \frac{1}{2} \int_{T_C}^{T} \left[\tilde{r}_m(t - T_C) + \tilde{r}_m(t) \right]^2 dt . \tag{5.38}$$

When a bit "0" is transmitted then, according to (5.29) and (5.30), the

transmitted energy occupies only the odd subspace. Applying the steps discussed above, the energy received in the odd subspace is obtained as

$$E_2 = \frac{1}{2}\int_{T_C}^{T} [-\tilde{r}_m(t - T_C) + \tilde{r}_m(t)]^2 \, dt \,. \tag{5.39}$$

The decision is done in favor of bit "1" if

$$E_1 > E_2 \qquad \text{or} \qquad E_1 - E_2 > 0 \,. \tag{5.40}$$

In FM-DCSK $T_C = T/2$. Substituting (5.38) and (5.39) into (5.40), the autocorrelation detection algorithm is obtained. The decision is done in favor of bit "1" if

$$\int_{T/2}^{T} \tilde{r}_m(t - T/2)\tilde{r}_m(t)dt > 0 \,. \tag{5.41}$$

The block diagram of autocorrelation detector constructed from (5.41) is shown in Fig. 5.9. Note, the autocorrelation detector determines the sign of correlation measured between the reference and information bearing chips, and the decision is done according to the sign of correlation. The only *a priori* information exploited by the detector is the sign of correlation. Because of the minimum amount of *a priori* information exploited, the autocorrelation detector has the worse noise performance [11].

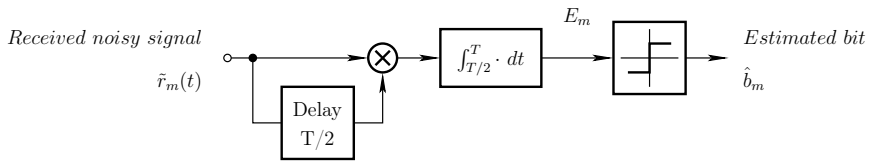

FIGURE 5.9
Block diagram of autocorrelation detector.

5.5 Implementation of a Microwave FM-DCSK System

Although a lot of materials have been published on chaotic communications systems, each of them uses only computer simulations to verify the results derived and the feasibility of chaos-based communications. The reason is very simple, the modulation schemes and demodulation algorithms required in chaotic communications are completely different from those used in conventional communications, hence, the integrated circuits developed for

conventional radio communications cannot be used to implement a chaotic transceiver.

The advent of SDE has made the implementation of chaotic communication systems easy and possible. In the SDE approach (i) the entire transceiver is implemented in baseband and (ii) a universal RF hardware device is used to reconstruct the analog microwave/RF signal from its complex envelope and to extract the complex envelope from the received microwave/RF signal at the transmitter and receiver, respectively.

Bandpass microwave/RF signals are used in radio communications where, typically, the center frequency of modulated signal is much greater than its bandwidth. These signals can be *fully represented* without any distortion in BB by their complex envelopes [8]. The complex envelope is a complex-valued signal, its real and imaginary parts are referred to as the I/Q components of BB signals. The I/Q components are *lowpass signals* and their bandwidth is equal to the half of the bandwidth of RF bandpass signal. Hence, the sampling frequency required to process the BB signal is determined by the *bandwidth* of bandpass RF signal. The center frequency of RF bandpass signal has no influence on the required sampling rate, hence, the complex envelope concept assures the minimum sampling rate required.

The lowpass complex envelopes, i.e., the BB equivalent signals, are digitized and processed by a host computer or FPGA and the entire transceiver is implemented in SW.

This technology is used here to demonstrate the feasibility of an FM-DCSK microwave radio transceiver. The details of SDE approach and the derivation of BB equivalents are not discussed here, for details refer to [15].

5.5.1 HW platform of implementation: The USRP device

The Universal Software Radio Peripheral (USRP) device [2] is a computer-hosted hardware platform developed for the implementation of software defined radio or low-accuracy virtual instrumentation. Each USRP device includes a receive and a transmit block. These blocks are used to generate the BB signals from the received RF one in the receive block and to reconstruct the RF bandpass signal from its BB equivalent in the transmit block. The USRP device performs all the waveform-specific signal processing tasks (such as modulation and demodulation) in BB on a host-computer while all the general purpose operations requiring high-speed data processing (such as interpolation and decimation) are carried out on an FPGA available on the main board of USRP device [15].

5.5.2 Software platform for accessing the USRP device

LabVIEW [1] is a data-flow type graphical programming software environment used to get access to the USRP device. It offers a graphical user interface and an icon-based graphical code development environment referred to as “Front

Panel" and "Block Diagram," respectively. LabVIEW platform provides icons to perform any kinds of signal processing tasks, data acquisition, even remote control of stand alone equipment.

The USRP device implements the physical layer in the OSI basic reference model, consequently, it has to offer two kinds of services for the host-computer: (i) USRP management service to set the USRP parameters such as receiver gain, carrier frequency, transmitted power, etc., and (ii) USRP data service to transfer the BB signal components. The former can be done via the configuration icons, while the latter is performed by the "Fetch I/Q Data" icon for the receive operation and "Write I/Q Data" icon for the transmit operation. The software implementation of the receive control chain is depicted in Fig. 5.10 where each icon is identified by its function shown above the icon.

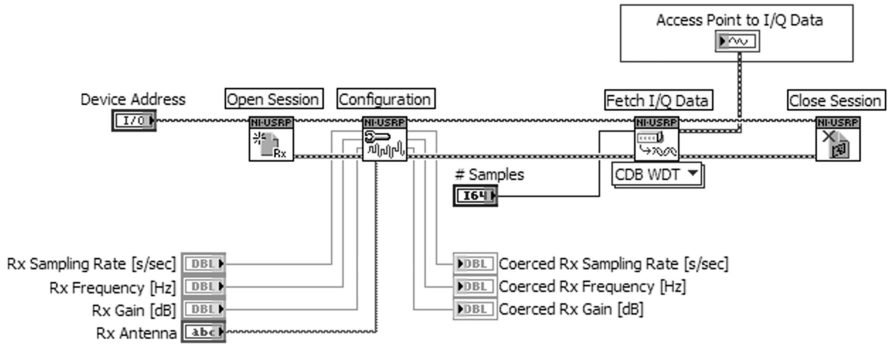

FIGURE 5.10
Complete control chain of the USRP device in receive mode.

The USRP devices are connected to the host computer via a Gigabit Ethernet interface and are identified by their IP addresses entered via the "Device Address" icon. This icon also opens the session with the USRP device. Then the following USRP parameters are entered via the "Configuration" icon:

- Rx Sampling Rate [s/sec]: Sample rate applied to the BB waveforms.
- Rx Frequency [Hz]: Assigns the RF center frequency.
- Rx Gain [dB]: Specifies the gain of RF amplifiers.
- Rx Antenna: Selects the transceiver configuration (duplex or simplex).

The USRP device keeps these parameters under control. If a desired combination of parameters is not allowed then the USRP device selects the closest parameter set available. These actual, referred to as "Coerced" parameters are returned by the "Configuration" icon. The "Fetch I/Q Data" icon uploads the digitized BB signal from the USRP device to the host-computer. It is also used to select the number of BB samples to be uploaded. Note, using the OSI terminology, this icon provides the access point to the I/Q components of BB

equivalent of received RF bandpass signal. Finally, the "Close Session" icon terminates the session with the USRP device.

5.5.3 Measured spectra of FM-DCSK signals

Recall, the spectra of an FM-DCSK signal carrying pure bit "1" and "0" sequences are completely separated in the frequency domain. The theoretical results concluded in (5.27)–(5.30) have been verified in Sec. 5.4.3 by computer simulations. The results of simulations are shown in Fig. 5.7.

To verify the results of theoretical investigations and the feasibility of chaotic radio communications by *measurements*, an FM-DCSK transceiver with an autocorrelation detector have been implemented using the USRP HW and LabVIEW SW platforms. The center frequency and data rate of implemented FM-DCSK radio system are 2.4 GHz and 500 kHz, respectively.

Figures 5.11(a) and 5.11(b) shows the spectra measured with a stand-alone microwave spectrum analyzer. The analyzer settings are shown in the figures. As expected from the theory, the spectra belonging to the pure bit "1" and "0" sequences are fully separated.

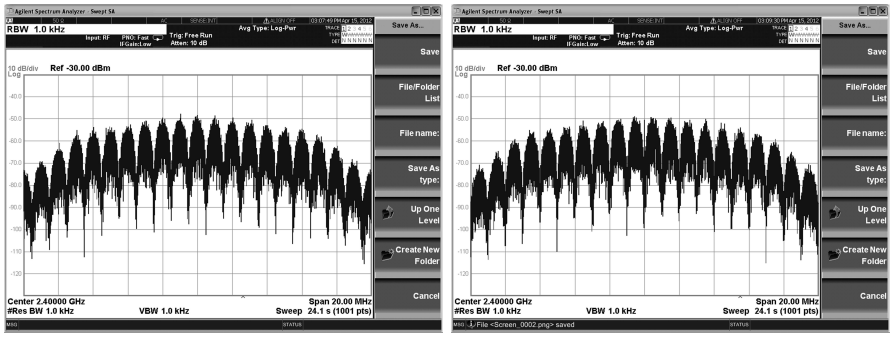

(a) (b)

FIGURE 5.11
Measured spectra of an 2.4-GHz FM-DCSK signal when (a) a pure bit "1" and (b) a pure bit "0" sequence is transmitted. The data rate is 500 kHz.

5.5.4 2.4-GHz FM-DCSK transceiver

The Front Panel of the implemented 2.4-GHz FM-DCSK transceiver is shown in Fig. 5.12. The configuration parameters of the USRP device are entered and the coerced parameter values are returned on the left side of the Front Panel. The bit duration T is also entered on the left subpanel.

The top left and right figures show I/Q components of BB signal in the time domain and the spectrum of BB signal when a random bit stream is

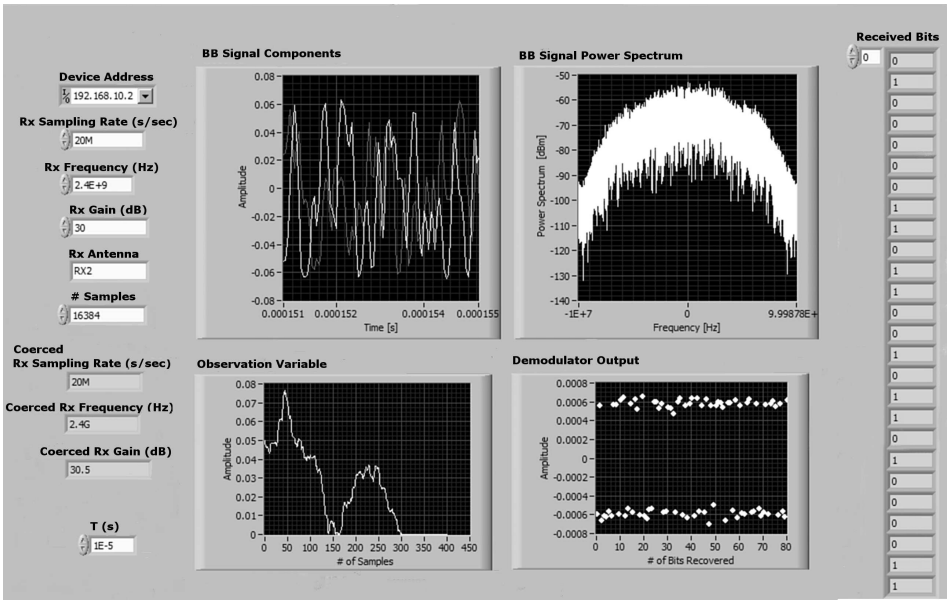

FIGURE 5.12
Front panel of the implemented FM-DCSK receiver.

received. The left figure in the bottom shows the observation signal generated by the autocorrelation detector. This signal, denoted by E_m in Fig. 5.9, is used by the timing recovery and decision algorithms to perform the demodulation.

The RF bandwidth of FM-DCSK signal, set to 17 MHz, is determined by the chaotic signal generator implemented by a Bernoulli map and by the FM modulator [9].

The bottom right plot shows the estimated, i.e., the demodulated bit stream which is denoted by $\hat{b}_m$ in Fig. 5.9. The received bit stream is visualized on the right side of the Front Panel.

The autocorrelation detector of Fig. 5.9 has been derived for the reception of a single isolated bit. To avoid InterSymbol Interference (ISI) the 2.4-GHz FM-DCSK receiver has been designed in such a way that the Nyquist ISI criterion is satisfied [8].

5.6 Conclusions

The waveform communications concept establishes a common framework for the description of any digital modulation scheme using either sinusoidal,

chaotic or random carriers. In waveform communications every symbol to be transmitted is mapped into an analog waveform of finite duration.

The most important feature of chaotic communications is that the transmitted signal is never periodic, instead, it is continuously varying even if the same symbol is transmitted repeatedly.

Transmitted waveforms are constructed from basis functions. Unfortunately, chaotic basis functions are orthonormal only in mean. This leads to the auto- and cross-correlation estimation problems which, if not prevented, corrupt the BER performance of the chaotic communications system.

Chaotic signals have no amplitude, frequency or phase, consequently, the conventional modulation schemes cannot be used. The most popular chaotic modulation schemes are CSK, DCSK and FM-DCSK. Among them the FM-DCSK offers the best BER performance.

The mathematical framework that makes the derivation of detection algorithms possible is the received signal space which is a finite dimensional Hilbert space. Both the *a priori* information and the received signal are projected into the received signal space and the decision is done in favor of symbol that is the closest to the received signal.

To show the applicability of the theory developed, the derivation of coherent, averaged optimum noncoherent and autocorrelation detection algorithms and detector configurations have been shown.

Note, going from coherent detection algorithm to the autocorrelation one there is a continuous loss in *a priori* information exploited. The ability of a detector to suppress noise and interference depends on the amount of *a priori* information available and *exploited* by the detection algorithm. Hence, if only the noise performance and interference rejection capability are considered then the coherent and autocorrelation detectors offer the best and worst, respectively, system performance.

To verify the feasibility of chaotic communications, an FM-DCSK radio link operating in the 2.4-GHz ISM band has been implemented using the SDE approach. In the SDE approach each RF signal processing block including the modulator and demodulator is implemented in software and in the baseband, and a universal hardware device referred to as USRP is used to convert the signals between the RF domain and baseband.

Acknowledgments

The NI USRP devices and NI LabVIEW software used to implement the FM-DCSK radio link have been donated by the National Instruments. This work has been sponsored by the Hungarian Scientific Research Found (OTKA) under Grant number T-084045.

Bibliography

[1] LabVIEW System Design Software. *National Instruments*. Online: <http://www.ni.com/labview/>.

[2] NI Universal Software Radio Peripheral (USRP). *National Instruments*. Online: <http://sine.ni.com/nips/cds/view/p/lang/en/nid/209947>.

[3] B. L. Basore. *Noise-like signals and their detection by correlation*. PhD thesis, MIT, Cambridge, MA, 1952.

[4] J. S. Bendat and A. G. Piersol. *Measurement and Analysis of Random Data*. John Wiley & Sons, New York, 1966.

[5] H. Dedieu, M. P. Kennedy, and M. Hasler. Chaos shift keying: Modulation and demodulation of a chaotic carrier using self-synchronizing Chua's circuits. *IEEE Trans. Circuits and Syst. II*, 40(10):634–642, October 1993.

[6] Federal Communications Commission. *Part 15 of the Commission Rs Rules Regarding Ultra-Wideband Transmission Systems; Subpart F.* FCC–USA, Online: <http://sujan.hallikainen.org/FCC/FccRules/2009/15/>.

[7] M. Hasler, G. Mazzini, M. Ogorzalek, R. Rovatti, and G. Setti (Eds.), Special Issue on. Applications of Nonlinear Dynamics to Electronic and Information Engineering. *Proceedings of the IEEE*, 90(5), May 2002.

[8] S. Haykin. *Communication Systems*. John Wiley & Sons, 3rd edition, 1994.

[9] M. P. Kennedy, G. Kolumbán, G. Kis, and Z. Jákó. Performance evaluation of FM-DCSK modulation in multipath environments. *IEEE Trans. Circuits and Syst. I*, 47(12):1702–1711, December 2000.

[10] G. Kis and G. Kolumbán. Constraints on chaotic oscillators intended for communications applications. In *Proc. NOLTA'98*, pages 883–886, Crans-Montana, Switzerland, September 14–17 1998.

[11] G. Kolumbán. Theoretical noise performance of correlator-based chaotic communications schemes. *IEEE Trans. Circuits and Syst. I*, 47(12):1692–1701, December 2000.

[12] G. Kolumbán and M. P. Kennedy. The role of synchronization in digital communication using chaos—Part III: Performance bounds. *IEEE Trans. Circuits and Syst. I*, 47(12):1673–1683, December 2000.

[13] G. Kolumbán, M. P. Kennedy, Z. Jákó, and G. Kis. Chaotic communications with correlator receiver: Theory and performance limit. Invited paper in *Proceedings of the IEEE*, 90(5):711–732, May 2002.

[14] G. Kolumbán, G. Kis, Z. Jákó, and M. P. Kennedy. FM–DCSK: A robust modulation scheme for chaotic communications. *IEICE Transactions on Fundamentals of Electronics, Communications and Computer Sciences*, E81-A(9):1798–1802, Oct. 1998.

[15] G. Kolumbán, T. Krébesz, and F. C. M. Lau. Theory and application of software defined electronics: Design concepts for the next generation of telecommunications and measurement systems. *IEEE Circuits and Systems Magazine*, 12(2):8–34, Second Quarter 2012.

[16] G. Kolumbán, F. C. M. Lau, and C. K. Tse. Generalization of waveform communications: The Fourier analyzer approach. *Circuits, Systems and Signal Processing*, 24(5):451–474, September/October 2005.

[17] G. Kolumbán and B. Vizvári. Nonlinear dynamics and chaotic behaviour of the analog phase-locked loop. In *Proc. NDES'95*, pages 99–102, Dublin, Ireland, July 1995.

[18] G. Kolumbán, B. Vizvári, W. Schwarz, and A. Abel. Differential chaos shift keying: A robust coding for chaos communication. In *Proc. NDES'96*, pages 87–92, Seville, Spain, June 27–28, 1996.

[19] T. S. Parker and L. O. Chua. *Practical Numerical Algorithms for Chaotic Systems*. Springer Verlag, New York, 1989.

[20] U. Parlitz, L. O. Chua, Lj. Kocarev, K. S. Halle, and A. Shang. Transmission of digital signals by chaotic synchronization. *Int. J. Bif. Chaos*, 2:973–977, 1992.

[21] J. G. Proakis. *Digital Communications*. McGraw-Hill, Singapore, 1995.

[22] K. Siwiak and D. McKeown. *Ultra-Wideband Radio Technology*. Wiley, Chichester, UK, 2004.

[23] R. van Nee and R. Prasad. *OFDM for Wireless Multilmedia Communications*. Artech House Publishers, Artech House Publishers, 2000.

Index